Available online at www.sciencedirect.com
SCIENCE DIRECT®
Journal of Sound and Vibration 266 (2003) 645–654
JOURNAL OF SOUND AND VIBRATION
www.elsevier.com/locate/jsvi

Double adaptive notch filter for mechanical grain flow sensors

K. Maertens[a,*], P. Reyns[a], J. De Baerdemaeker[a]

[a] *Laboratory for Agro-Machinery and Processing, Catholic University Leuven, Kasteelpark Arenberg 30, 3001 Leuven, Belgium*

Received 13 January 2003

Abstract

Nowadays, commercial combine harvesters are equipped with special sensors for the purposes of precision farming. Sensors are installed to measure the harvested surface and mass flow each second. Hence, grain yield maps are constructed, approximating the actual grain yield on the field before harvesting.

Most grain flow sensors are installed on the paddle elevator before storage in the grain tank. At the elevator exit, paddles throw packs of grain against a curved plate on which a force transducer is attached. Therefore, the measured flow signal is heavily disturbed by the paddle rate and resonance frequency of the mechanical sensor.

In this study, a computationally cheap method is presented to track both frequencies in the measured flow signal. Based on these frequency trackers, a double notch filter is tuned continuously to remove both disturbances. Moreover, the knowledge about the frequency content can be used to monitor the condition of the mechanical sensor and the paddle elevator.

1. Introduction

Extensive research has focused on measuring grain flow of combine harvesters for many years. First, sensors have been developed for purposes of automation [1]. The grain flow at the end of the separation process is directly related to the total feedrate of the machine and consequently to its internal state. Later on, techniques for site-specific management have been introduced and accordingly, the interest for site-specific grain yield has grown. Nowadays, each type of combine harvester can be bought with its own device for measuring grain yield online.

*Corresponding author.
E-mail address: koen.maertens@agr.kuleuven.ac.be (K. Maertens).

0022-460X/$ - see front matter
doi:10.1016/S0022-460X(03)00590-X

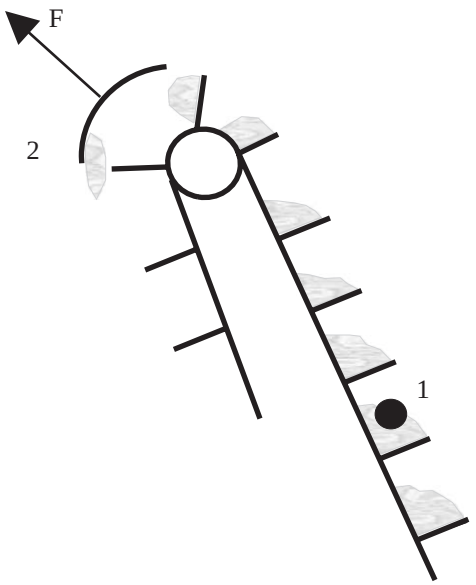

Fig. 1. Set-up of two different grain flow measurements on a paddle elevator: a volumetric flow measurement (1) based on the interruption time of an optical beam and a force measurement (2) of the impulse moment on a circular chute.

To measure the mass flow of bulk solids online, a clean, stationary and continuous flow is desirable. Therefore, grain flow units are installed on the paddle elevator of the combine harvester (Fig. 1), after the flow has been cleaned from chaff and short straw.

In practice, the most used types of grain flow measurements are:

(1) Volumetric flow measurements [1], based on the interruption time of an optical beam transmitted through the elevator. To estimate local yield, extra parameters must be introduced to compensate for variations in volumetric weight and field slopes.
(2) Impact or impulse flow sensors, placed at the outlet of the elevator. Since the mass flow itself is measured and the mechanical sensor is balanced no extra terms for correction are needed. A circular chute must be put at the exit of the elevator to generate an impulse flow. In conditions of high and wet grain flows (e.g. corn), material can get stuck on the plate, causing damage and implying wrong measurements.

In this study, an impulse flow sensor [2] is installed on a New Holland TX64 combine harvester.

2. Frequency content of grain flow signal

The result of a grain flow measurement at a sample rate of 125 Hz is shown in Fig. 2. Two large peaks are appearing in the power spectrum. The first peak at 13.2 Hz corresponds to the first mode of the mass flow sensor and remains constant for normal working conditions. A second

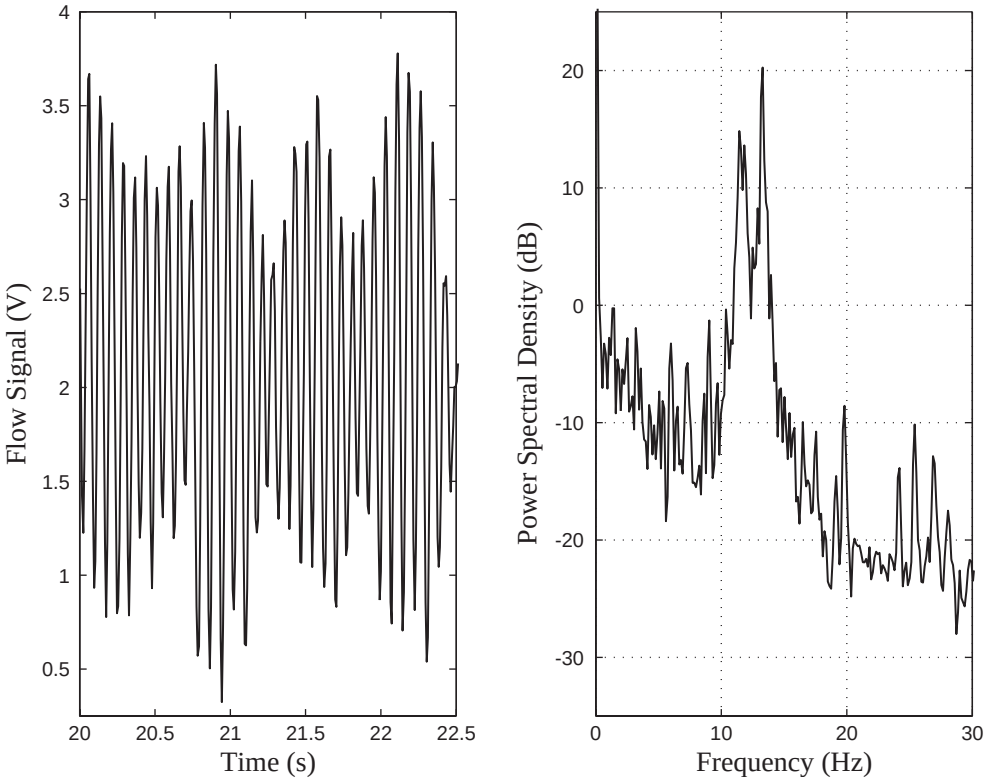

Fig. 2. Time and frequency domain representation of grain flow signal.

peak is present around 11.6 Hz. The latter comes from the pulsewise supply of grain flow to the sensor and corresponds with the paddle rate. This frequency is not constant but varies slightly due to elevator speed variations.

Classically, the above spectrum is handled by means of an analogous Butterworth filter to guarantee a minimized ripple in the pass band. Most commercial systems operate at a sample rate of 1 Hz, hence a second order filter is sufficient to remove the effects of aliasing.

When higher sample rates are desired, special measures must be taken. For stationary disturbances, a double notch filter in cascade with a low order filter would be sufficient to remove both frequencies. In this case, both disturbing frequencies will vary. A frequency tracking algorithm must be introduced to adapt the double notch filter continuously.

3. Rejection of sinusoidal disturbances

After an introduction about the design of multiple notch filters, an adaptive algorithm is presented to track and correct both disturbance frequencies.

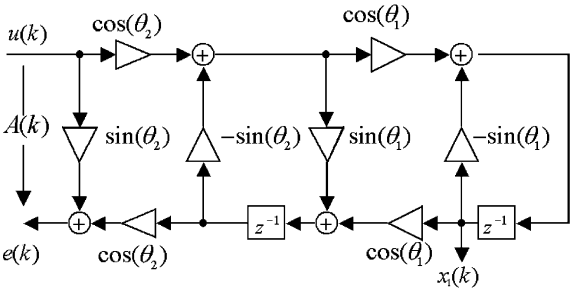

Fig. 3. Normalized second order lattice filter.

3.1. Design of multiple notch filter

The ideal notch filter $F_{notch}(\mathrm{j}\omega)$ can be defined by[1]

$$F_{notch}(\mathrm{j}\omega) = \begin{cases} 0, & \omega = \omega_i, \\ 1, & \omega \neq \omega_i, \end{cases} \tag{1}$$

where the $\{\omega_i\}$ denote the different notch frequencies. The standard way to approximate the ideal notch characteristic is given by

$$F(z^{-1}) = \frac{N(z^{-1})}{N((z/\rho)^{-1})} \quad (0 \ll \rho < 1). \tag{2}$$

The numerator $N(z^{-1})$ places zeros on the unit circle accordingly to each notch frequency $\{\omega_i\}$. Two poles are put on the same frequency lines but with a range ρ. This parameter defines the gain and 3-dB bandwidth B (Hz). For low 3-dB bandwidths and by this, poles near the unit circle, numerical problems can arise when different single notch filters are placed in cascade.

In Ref. [3] an alternative approach is formulated based on all-pass filters:

$$F(z^{-1}) = 0.5\{1 + A_{2N}(z^{-1})\}. \tag{3}$$

An all-pass filter $A_{2N}(z^{-1})$ of $2N$th order is determined by a cascade of second order all-pass filters (Fig. 3):

$$A_{2N}(z^{-1}) = \prod_{i=1}^{N} \frac{(\sin\theta_{2i} + \sin\theta_{1i}(1 + \sin\theta_{2i})z^{-1} + z^{-2})}{(1 + \sin\theta_{1i}(1 + \sin\theta_{2i})z^{-1} + \sin\theta_{2i}z^{-2})}. \tag{4}$$

Parameters $\{\theta_{1i}\}$ and $\{\theta_{2i}\}$ are respectively defined by

$$\theta_{1i} = \omega_i - \pi/2, \tag{5}$$

$$\sin(\theta_{2i}) = \frac{(1 - \tan(B_i/2))}{(1 + \tan(B_i/2))}. \tag{6}$$

[1] Frequencies and bandwidths are normalized between 0 and 2π.

3.2. Adaptive correction

From Eq. (5), the parameters $\{\theta_{1i}\}$ are directly related to the frequency of the sinusoidal disturbances. Since these frequencies are time-varying, an adaptive algorithm must be introduced. Here, bandwidth parameters $\{\theta_{2i}\}$ are kept constant.

3.2.1. Single adaptive notch filter

To tune the notch frequency parameter θ_1, the following algorithm has been proposed by Regalia [4]:

$$\theta_1(k+1) = \theta_1(k) - \mu(k)e(k)x_1(k) \tag{7}$$

with $\mu(k)$ a positive gain sequence, $e(k)$ and $x_1(k)$, respectively, the output and regressor signal of Fig. 3. Different choices can be made for the gain sequence. In this study, the gain sequence is kept constant. A larger gain will result in a higher capability for tracking frequency variations. A lower gain will bring about a frequency estimator with lower variance.

Assuming that the flow signal can be approximated by

$$u(k) = v(k) + a_1\cos(\omega_1 k + \phi_1) + a_2\cos(\omega_2 k + \phi_2) \tag{8}$$

with $v(k)$ denoting a white-noise process.

The algorithm's behaviour can be explained through averaging analysis. The frequency tracking in the case of M multiple sinusoidal disturbances can be approximated by [4]

$$\frac{\mathrm{d}\theta_1(\tau)}{\mathrm{d}\tau} = -\sum_{i=1}^{M}\frac{a_i^2}{4\pi}\frac{\cos\theta_1(\tau)\cos\theta_2}{|D(\mathrm{e}^{-\mathrm{j}\omega_i}, \Theta(\tau))|^2}(\cos\omega_i + \sin\theta_1(\tau)), \tag{9}$$

$$\frac{\mathrm{d}\theta_1(\tau)}{\mathrm{d}\tau} = -\beta(\tau)\left[\sin\theta_1(\tau) + \sum_{i=1}^{M} c_i(\Theta(\tau))\cos\omega_i\right], \tag{10}$$

where

$$\beta(\tau) = \cos\theta_2\cos\theta_1(\tau)/4\pi\sum_{i=1}^{M} a_i^2/|D(\mathrm{e}^{-\mathrm{j}\omega_i}, \Theta(\tau))|^2, \tag{11}$$

$$c_i(\tau) = \frac{a_i^2/|D(\mathrm{e}^{-\mathrm{j}\omega_i}, \Theta(\tau))|^2}{\sum_{l=1}^{M} a_l^2/|D(\mathrm{e}^{-\mathrm{j}\omega_l}, \Theta(\tau))|^2}\ (>0). \tag{12}$$

The denominator $D(z^{-1}, \Theta(\tau))$ corresponds to the denominator of a single all-pass filter given by Eq. (4) ($N = 1$) and $\Theta(\tau)$ with a time-varying matrix of $\{\theta_{1i}(\tau), \theta_{2i}\}$. Since $\beta(\tau)$ is strictly positive in normal conditions ($|\theta_1(\tau)| < \pi/2$ and $|\theta_2(\tau)| < \pi/2$), the instantaneous attractor point is defined by the second term of Eq. (10).

Studies based on the design of appropriate Lyapunov functions [4,5] have proven the existence of local attractor points near each frequency for a narrow bandwidth B ($\theta_2 \to \pi/2$). Once the system has reached the neighbourhood of the attractor points, stability is guaranteed in case of smooth frequency variations.

Fig. 4 illustrates this behaviour for two sinusoidal disturbances corresponding to the measured grain flow signal of Fig. 2. The disturbance frequencies lie on 11.6 and 13.2 Hz. Figs. 4A–C show

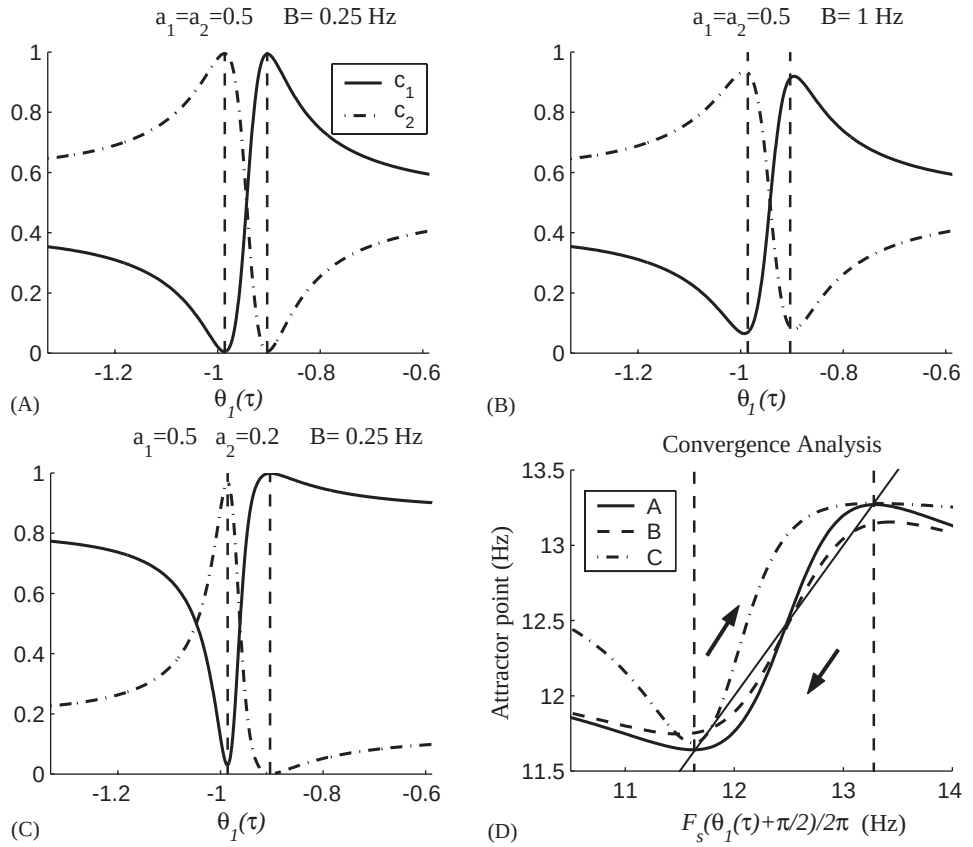

Fig. 4. Convergence analysis of single adaptive notch filter with two sinusoidal disturbances. (A–C) are illustrating the influence of amplitudes $\{a_i\}$ and bandwidth B on $c_i(\theta_i(\tau))$-weights. (D) shows the relation between the instantaneous frequency estimation and the corresponding attractor frequency.

the variations of the c_i-weights as function of $\theta_1(\tau)$ for different disturbance amplitudes and notch bandwidth B. The position of the instantaneous attractor point $F_a(\tau)$(Hz) is plotted in Fig. 4D and calculated by means of

$$F_a(\tau) = F_s\left[\arcsin\left(-\sum_{i=1}^{2} c_i(\tau)\cos\omega_i\right) + \pi/2\right] \Big/ 2\pi. \tag{13}$$

Three curves corresponding to the configuration of Figs. 4A–C are compared. A solid line is drawn to separate the direction of attraction. Points on curves in the upper-left corner result in increasing frequency estimates. Points in the bottom-right corner bring about decreasing frequency estimations. The parameter values are transformed into frequency units to simplify physical interpretation.

- In the case of a large bandwidth B comparing to the difference between both disturbance frequencies, the c_i-coefficients do not become perfectly one (Fig. 4B) on the corresponding frequency points ω_i, resulting in a biased frequency estimation (Fig. 4D).

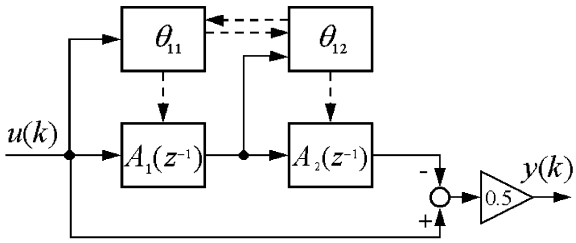

Fig. 5. Bidirectional parameter flow, realizing a robust, double adaptive notch filter.

- The presence of a strong sinusoidal disturbance in the immediate neighborhood of the aimed one, introduces problems of convergence and bias terms (Figs. 4C and D). In the case of configuration C, a slight perturbation of the θ_1-estimation around the weak frequency will let the tracking algorithm converge towards the other, stronger frequency (Fig. 4D).

3.2.2. Double adaptive notch filter

Both frequency peaks in Fig. 2 provide valuable information about the system. Therefore, each frequency should be tracked in a robust way, avoiding problems of convergence. Fig. 5 illustrates how convergence can be guaranteed by means of a bidirectional connection between both tracking algorithms. The cascaded connection of Ref. [4] induces parameter $\theta_{12}(k+1)$ to follow the weaker paddle rate after the resonance frequency is first filtered out by means of a second order notch filter on the previous calculated $\theta_{11}(k+1)$. In this study, an analogous correction is added in the other direction where the previous estimated $\theta_{12}(k)$ is used to filter the input signal of the $\theta_{11}(k+1)$-estimation.

The effect on the stability of both frequency trackers can be derived from Fig. 4D. By filtering out one frequency before the other one is estimated, the convergence region is expanded. This effect is visible by comparing the tracking convergence for the 13.2 Hz frequency component. Plot A corresponds to the case of two disturbance frequencies with equal strength. When the amplitude of the second frequency at 11.6 Hz is lowered by a factor of 2.5, plot C is obtained. A significant larger convergence zone around 13.2 Hz is achieved. When the same can be done for the other frequency tracker, the performance of the double frequency tracker is significantly improved.

4. Results

To analyse the tracking capability of the algorithm, simulations are performed using *Matlab*. As input signal, two sinusoidal disturbances are generated with nominal frequencies of 13.2 and 11.6 Hz and amplitudes of respectively 0.5 and 0.27. Gaussian white noise is added with a power spectrum of -10 dB. Bandwidths B_i are set to 0.5 Hz and each simulation is initialized with $\theta_{11}(0)$- and $\theta_{12}(0)$-values corresponding with initial frequencies of 14.5 and 10.5 Hz. The gain sequence μ_1 of the θ_{11}-estimator is set at a constant value of 0.5×10^{-4}. The gain μ_2 is set at a constant value of 10^{-5}. These parameter values are found to be optimal for measured grain flow signals.

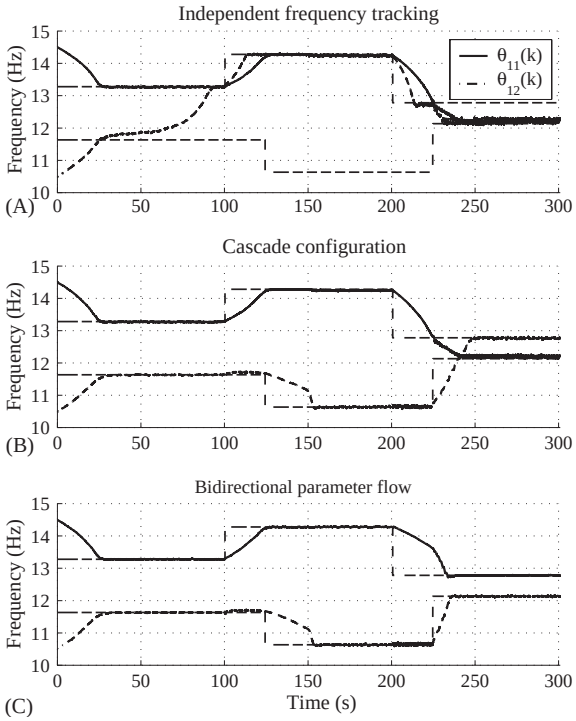

Fig. 6. Simulation results for three realizations of a double notch filter: (A) two independent frequency estimators; (B) unidirectional cascade configuration [4]; (C) bidirectional parameter correction (Fig. 5).

Fig. 6 shows the results of three double adaptive notch filters. Each disturbance frequency varies two times during the simulation. At 150 s, the amplitude of the paddle rate disturbance is amplified by a factor of 2.5 and becomes slightly stronger than the resonance frequency. The three plots of Fig. 6 correspond with following configurations:

(1) Two tracking algorithms are estimating the frequencies independently. The resulting $\{\theta_{1i}(k)\}$ and $\{\theta_{2i}\}$ are implemented in the adaptive all-pass filter of Eq. (4) and applied to the input signal.

As could be expected from the stability analysis of Fig. 4D, no stable tracker for the weaker paddle rate frequency is found. Already at the initialization of the notch filter, the second frequency estimator converges towards the strongest frequency. After time step 150, the paddle frequency is followed.

(2) As proposed in Ref. [4], the strongest disturbance is estimated first. Subsequently, a second order notch filter $(0.5\{1 - A_1(z^{-1})\})$ is placed on this frequency and the second frequency is estimated.

During the first part of the simulation, both frequency estimators converge consistently to the effective disturbance frequencies of the system. As long as the power of the resonance frequency dominates the paddle rate, no problems arise. After the amplification of a_2, the θ_{11}-estimation keeps following the strongest with a small bias term. The θ_{12}-tracker follows consistently the weakest disturbance.

(3) Before estimation of the first notch frequency $\{\theta_{11}(k+1)\}$, the latest estimation of the other frequency $\{\theta_{12}(k)\}$ is used in a second order notch filter and vice versa (see Fig. 5). As a result, the interesting properties of the case of one single sinusoidal disturbance are approximated for both frequency estimations.

The simulation shows how these properties are fulfilled by the tracking algorithm. Each tracker follows its disturbance frequency and no bias terms arise on the estimated frequencies.

The third configuration is applied to effective measured grain flow signals with the settings and initialization of the previous simulation. The results in time and frequency domains are shown in Fig. 7 together with the estimated frequencies and a nominal frequency characteristic (notch on 11.6 and 13.2 Hz). Both in the time and frequency domains, the influence of the adaptive notch filter on the measured signal is clearly visible. The largest peak is decreased with 10 dB. As a result, a fixed second order Butterworth filter can be used to register the grain flow at a sample rate of 5 Hz. Since the grain flow signal does not exhibit a constant power spectrum outside the disturbance frequencies, some low frequency ripples are present in the frequency trajectories.

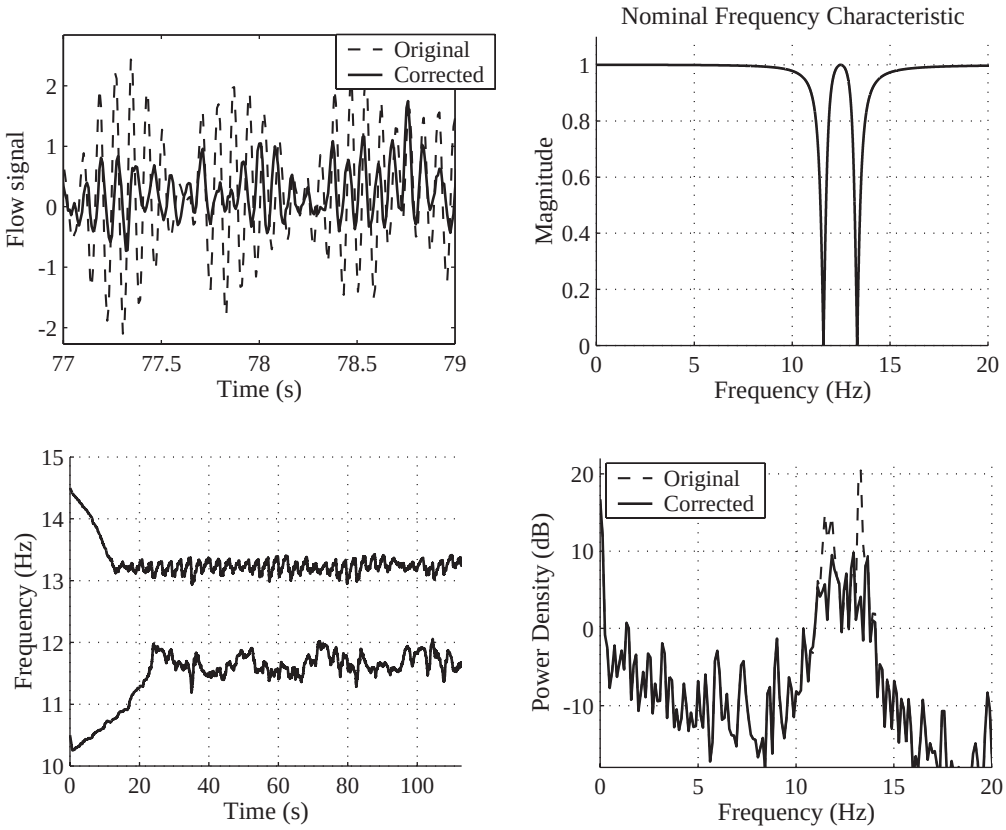

Fig. 7. Application of a bidirectional, double adaptive notch filter on a measured grain flow signal.

5. Conclusions

In this paper, a method is introduced to track the main sinusoidal disturbances on a mechanical grain flow sensor placed at the end of a paddle elevator. Due to a bidirectional parameter exchange between both frequency tracking algorithms (see Fig. 5), robustness and consistency are guaranteed for both frequency estimations which provide interesting information about the condition of the mechanical sensor and paddle elevator. The same algorithm can be expanded for extra sinusoidal disturbances.

Computationally, the algorithm is cheap since it is based on an algebraic correction (Eq. (7)) and the design of a low order all-pass filter. No matrix inversion or Fourier transformation is necessary.

Acknowledgements

The authors gratefully acknowledge the I.W.T. (Instituut voor Wetenschappelijk Technologisch onderzoek) for the financial support through doctoral grant No. 003249. This study has been made possible with the cooperation of New Holland Belgium.

References

[1] N. Diekhans, Automatisierung am Mähdrescher, *Grundlagen der Landtechnik* 35 (4) (1985) 111–118.
[2] G. Strubbe, Mechanics of Friction Compensation in Mass Flow Measurements of Bulk Solids, Ph.D. Thesis, Department of Mechanical Engineering, Catholic University Leuven, 1997.
[3] P.A. Regalia, K. Mitra, P.P. Vaidyanathan, The digital all-pass filter: a versatile signal processing building block, *Proceedings of the IEEE* 76 (1988) 19–37.
[4] P.A. Regalia, An improved lattice-based adaptive IIR notch filter, *IEEE Transactions on Signal Processing* 39 (9) (1991) 2124–2128.
[5] M. Bodson, S.C. Douglas, Adaptive algorithm for the rejection of sinusoidal disturbances, *Automatica* 33 (12) (1997) 2213–2221.